Supporting Information

Boron phosphide as an efficient metal-free catalyst for nitrate electroreduction to ammonia

Nana Zhang [1#], Guike Zhang [1#], Ye Tian [2], Yali Guo [1], Ke Chu [1*]

[1] *School of Materials Science and Engineering, Lanzhou Jiaotong University, Lanzhou 730070, China*

[2] *Department of Physics, College of Science, Hebei North University, Zhangjiakou 075000, Hebei, China*

*Corresponding author. E-mail address: chuk630@mail.lzjtu.cn (K. Chu)

[#] These authors contributed equally to this work.

Experimental Section

Synthesis of BP

BP was synthesized based on a vacuum-sealed strategy. A mixture of B and P powders (B:P molar ratio: 1:1.2) with a total weight of 200 mg was placed in a silica tube which was vacuum-sealed. The sealed silica tube was then thermally annealed in a muffle furnace at 1000 ^{o}C for 10 h. Afterwards, the as-prepared powder was washed with 0.1 M HCl and deionized water to remove impurities, obtaining BP.

Electrochemical measurements

Electrochemical measurements were carried out on a CHI-760E electrochemical workstation with a standard three-electrode system, where catalyst coated on carbon cloth (CC, 0.5 mg cm^{-2}) was used as working electrode, graphite rod as counter electrode and Ag/AgCl as reference electrode. All potentials were referenced to reversible hydrogen electrode (RHE) according to the equation: E (V vs. RHE) = E (V vs. Ag/AgCl) + 0.198 V + 0.059 × pH. The NO_3RR measurements were carried out in 0.5 M Na_2SO_4 + 0.1 M $NaNO_3$ electrolyte using an H-type two-compartment electrochemical cell separated by a Nafion 211 membrane. Prior to NO_3RR electrolysis, the cathodic compartment was purged with Ar for 30 min. After each chronoamperometry test for 1 h, the produced NH_3 and other possible by-products (NO_2^- and N_2H_4) were analyzed by various colorimetric methods using UV-vis absorbance spectrophotometer (MAPADA P5), while the gas products were analyzed by gas chromatography (Shimadzu GC2010).

Determination of NH_3

NH_3 in electrolyte was quantitatively determined by the indophenol blue method[1]. The electrolyte was collected and diluted to the detection range. Coloring solution was prepared by dissolving $C_7H_6O_3$ (5 wt.%), $C_6H_5Na_3O_7$ (5 wt.%), NaClO (1 mL, 0.05 M) and $C_5FeN_6Na_2O$ (0.2 mL, 1wt.%) in 2 mL NaOH solution (1 M). Then, the coloring solution was added to 2 mL diluted electrolyte. After the incubation for 2 h at room temperature, the mixed solution was subjected to UV-vis measurement using the absorbance at 655 nm wavelength. The concentration-

absorbance curves were calibrated by the standard NH_4Cl solution with a series of concentrations, and the NH_3 yield rate and NH_3-Faradaic efficiency were calculated by the following equation[2]:

$$\mathrm{NH_3\ yield}\ (\mu\mathrm{g\ h^{-1}\ mg_{cat.}^{-1}}) = \frac{c_{\mathrm{NH_3}} \times V}{t \times A} \tag{1}$$

$$\mathrm{NH_3\text{-}Faradaic\ efficiency}\ (\%) = \frac{8 \times F \times c_{\mathrm{NH_3}} \times V}{17 \times Q} \times 100\% \tag{2}$$

where c_{NH3} (μg mL^{-1}) is the measured NH_3 concentration, V (mL) is the volume of the electrolyte, t (h) is the reduction time, A (cm^{-2}) is the surface area of CC (1×1 cm^2) , F (96500 C mol^{-1}) is the Faraday constant, Q (C) is the quantity of applied electricity.

Determination of NO_2^-

NO_2^- in electrolyte was quantitatively determined by a Griess test[3]. The electrolyte was collected and diluted to the detection range. Coloring solution was prepared by dissolving N-(1-naphthyl) ethylenediamine dihydrochloride (0.2 g), p-aminobenzenesulfonamide (4.0 g) and H_3PO_4 (10 mL, ρ = 1.685 g mL^{-1}) in 50 ml deionized water. Then, 0.2 mL coloring solution was added to 2 mL diluted electrolyte. After the incubation for 20 min at room temperature, the mixed solution was subjected to UV-vis measurement using the absorbance at 540 nm wavelength. The concentration-absorbance curves were calibrated by the standard KNO_2 solution with a series of concentrations.

Characterizations

X-ray diffraction (XRD) patterns were recorded on a Rigaku D/max 2400 diffractometer. X-ray photoelectron spectroscopy (XPS) analysis was performed on a PHI 5702 spectrometer. Transmission electron microscopy (TEM) and high resolution transmission electron microscopy (HRTEM) were performed on a Tecnai G^2 F20 microscope.

Calculation details

Density functional theory (DFT) calculations were carried out using a Cambridge sequential total energy package (CASTEP) with projector augmented wave pseudopotentials. The Perdew-Burke-Ernzerhof (PBE) generalized gradient

approximation (GGA) functional was used for the exchange-correlation potential. The DFT-D correction method was used to describe the van der Waals interactions throughout the calculations. The convergence tolerance was set to be 1.0×10^{-5} eV for energy and 0.02 eV $Å^{-1}$ for force. The Brillouin zones of the supercells were sampled by 4 × 4 × 1 uniform k point mesh, and a plane-wave basis set with an energy cut-off of 480 eV was employed. BP (111) was modeled by a 3×3 supercell, and a vacuum region of 15 Å was used to separate adjacent slabs.

The adsorption energy (ΔE) is defined as

$$\Delta E = E_{\mathrm{ads/slab}} - E_{\mathrm{ads}} - E_{\mathrm{slab}} \tag{3}$$

where $E_{\mathrm{ads/slab}}$, E_{ads} and E_{slab} are the total energies for adsorbed species on slab, adsorbed species and isolated slab, respectively.

The Gibbs free energy (ΔG, 298 K) of reaction steps is calculated by

$$\Delta G = \Delta E + \Delta ZPE - T\Delta S \tag{4}$$

where ΔE is the adsorption energy, ΔZPE is the zero-point energy difference and $T\Delta S$ is the entropy difference between the gas phase and adsorbed state. Given that it is difficult to directly calculate the energy of charged NO_3^-, the adsorption free energy of NO_3^- ($\Delta G(*NO_3)$) was calculated with assistance of the gaseous HNO_3 as follows[4]

$$\Delta G(*NO_3) = G(*NO_3) - G(*) - [G(HNO_3) - 0.5 \times G(H_2)] + \Delta G_{\mathrm{correct}} \tag{5}$$

where $G(*)$ and $G(*NO_3)$ are the Gibbs free energies of the bare catalyst and that with the adsorbed NO_3^-, respectively. $G(HNO_3)$ and $G(H_2)$ represent the Gibbs free energies of HNO_3 and H_2 molecule, respectively.

The Gibbs free energy of adsorption hydrogen atom is calculated by the following equation[5].

$$\Delta G{*}H = E[\mathrm{surface}+{*}H] - E[\mathrm{surface}] - 1/2E[H_2] + \Delta E_{\mathrm{ZPE}} - T\Delta S_H \tag{6}$$

where E[surface+H*] is the total energy of the system, including the adsorbed molecules and facet; E[surface] is the energy of the facet; $E(H_2)$ represents the total energy of a gas phase H_2 molecule; ΔE_{ZPE} denotes the zero-point energy of the system simplified as 0.05 eV; $-T\Delta S_H$ is the contribution from entropy at temperature K, which is taken as 0.20 eV at 298 K.

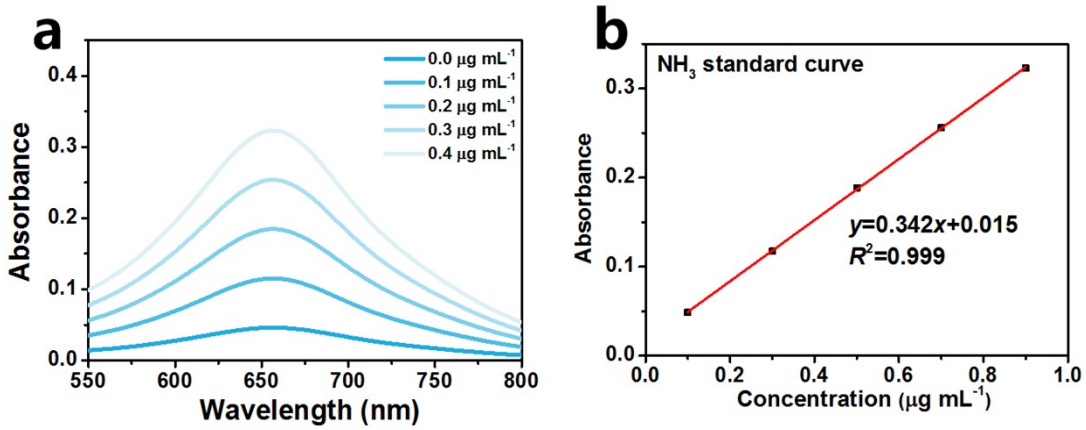

Fig. S1. (a) UV-vis absorption spectra of NH_4Cl assays after incubated for 2 h at ambient conditions. (b) Calibration curve used for the calculation of NH_3 concentrations.

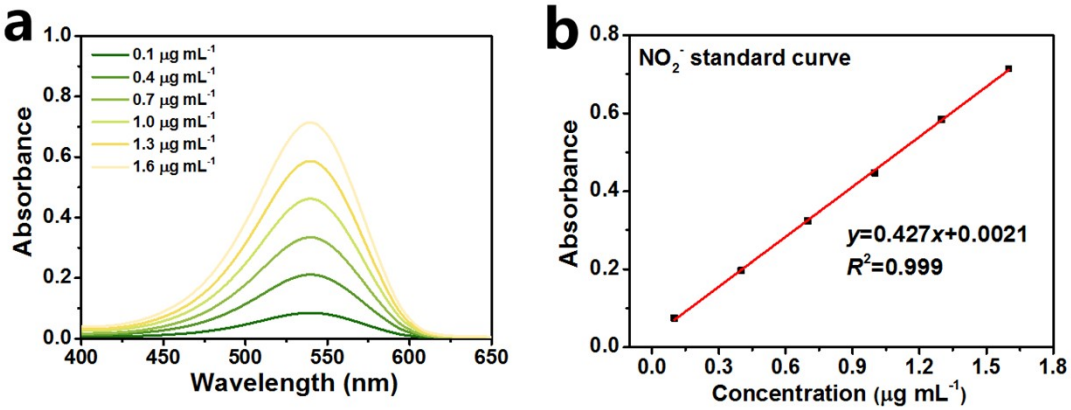

Fig. S2. (a) UV-vis absorption spectra of KNO_2 assays after incubated for 20 min at ambient conditions. (b) Calibration curve used for calculation of NO_2^- concentrations.

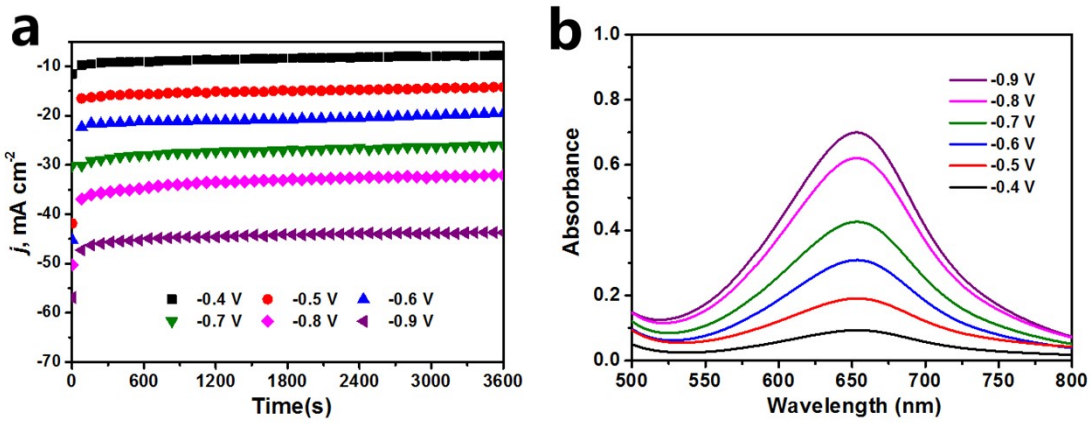

Fig. S3. (a) Potential-dependent chronoamperometry curve of BP after 1 h NO_3RR electrolysis, and corresponding (b) UV-vis spectra for detecting NH_3 (diluted by 50 times).

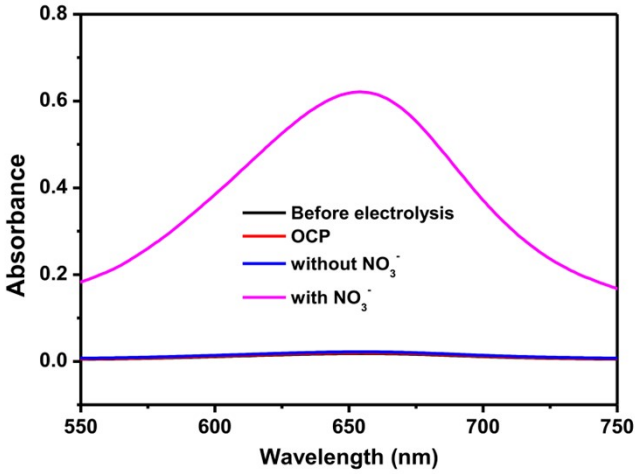

Fig. S4. UV-vis absorption spectra for detecting NH_3 in the electrolytes after 1 h NO_3RR electrolysis at different conditions (diluted by 50 times).

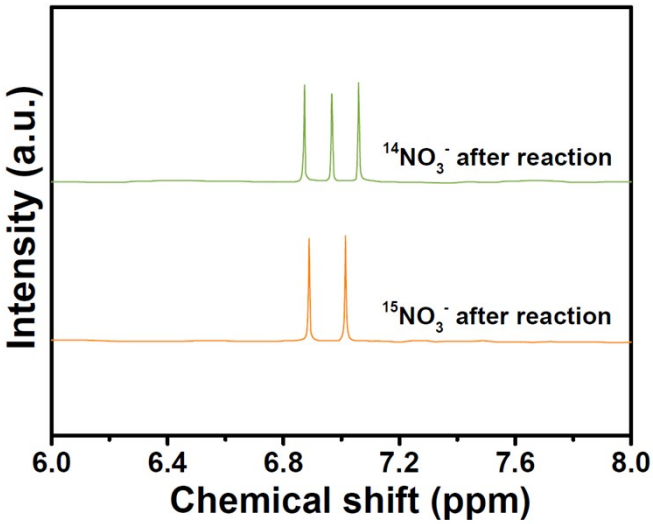

Fig. S5. ^{1}H NMR spectra of the electrolytes using $^{15}NO_3^-$ and $^{14}NO_3^-$ as nitrate sources.

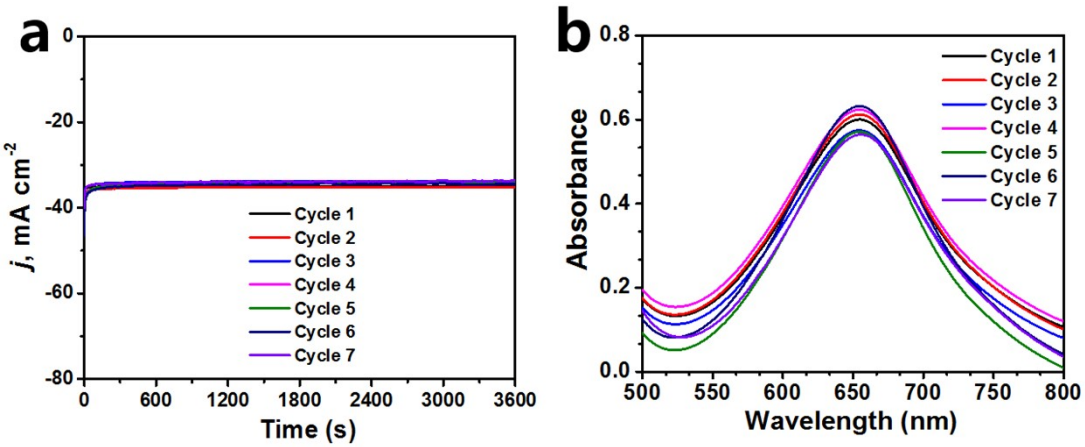

Fig. S6. (a) Potential-dependent chronoamperometry curve, and corresponding UV-vis absorption spectra for detecting NH_3 in the electrolytes after 1 h NO_3RR electrolysis at seven cycles (diluted by 50 times).

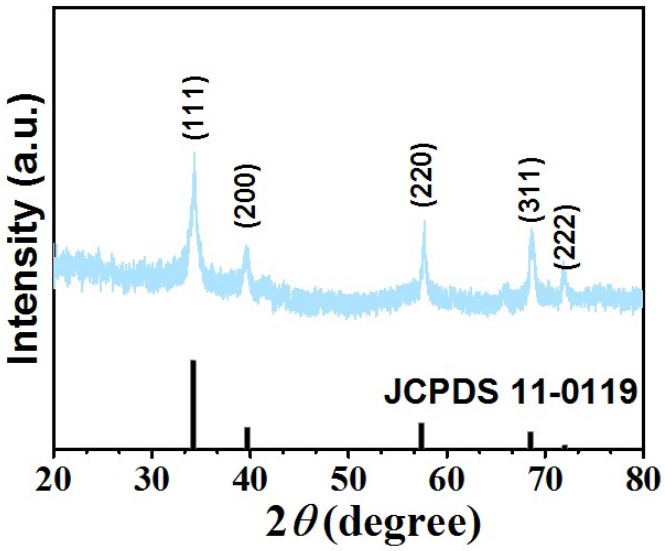

Fig. R7. XRD pattern of BP after stability test.

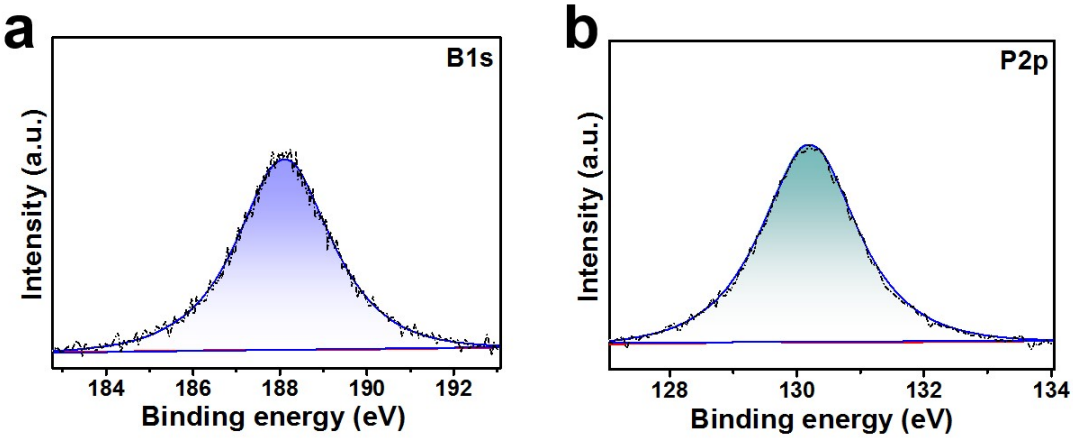

Fig. R8. XPS spectra of BP after stability test: (a) B1s, (b) P2p.

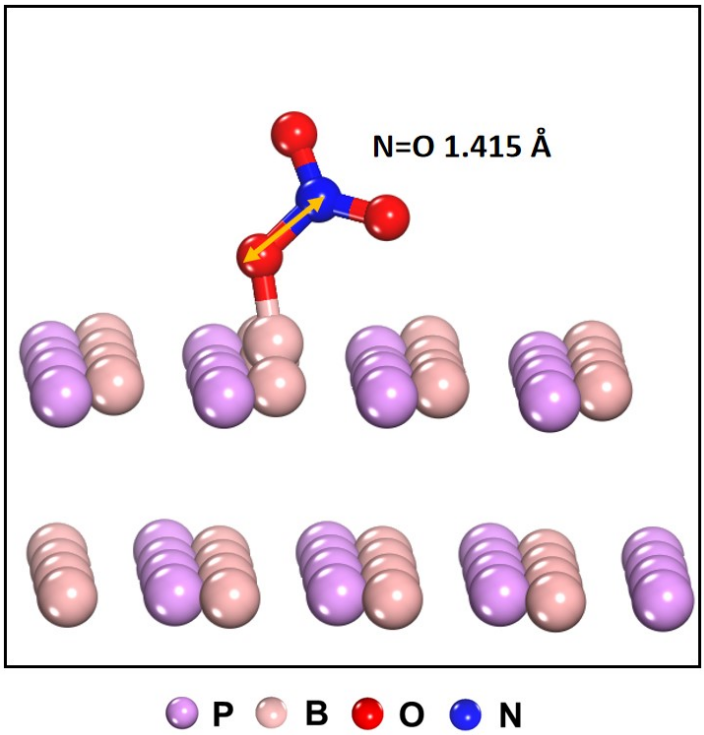

Fig. S9. Optimized structure of NO_3^- adsorption on BP.

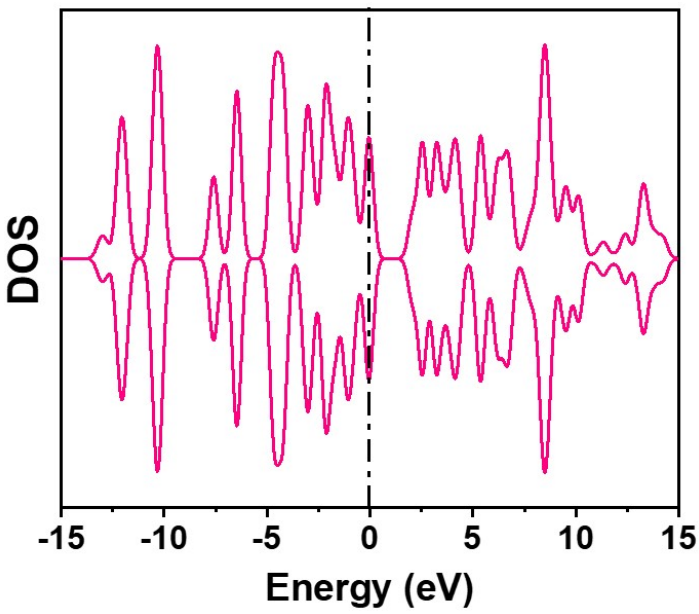

Fig. S10. DOS of bulk BP

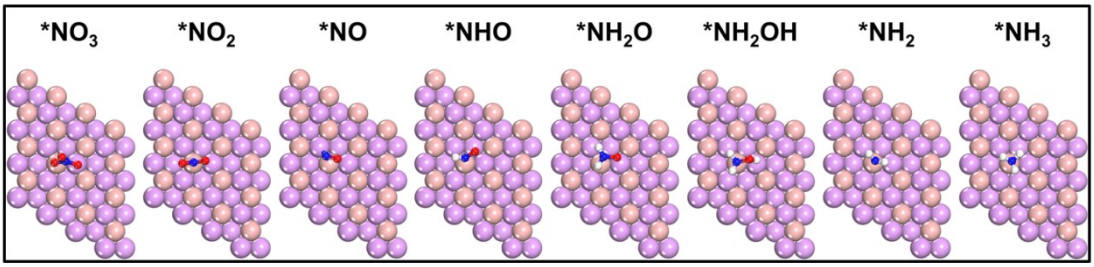

Fig. S11. Optimized adsorption configurations of the reaction intermediates in the NHO pathway on BP.

Table S1. Comparison of the optimum NH_3 yield and FE_{NH3} for the recently reported state-of-the-art NO_3RR electrocatalysts at ambient conditions.

Catalyst	Electrolyte	NH_3 yield rate (mg $h^{-1}cm^{-2}$)	FE_{NH3}(%)	Potential (V vs RHE)	Ref.
Fe-PPy SACs	0.1 M KOH （0.1 M KNO_3）	2.75	100	-0.7	[6]
Pd/TiO_2	1 M LiCl （0.25 M $K^{15}NO_3$）	1.12	92.1	-0.7	[7]
Ni_3B@$NiB_{2.74}$	0.10 M KOH （10 mM NO_2^-）	3.37	100	-0.3	[8]
a-RuO_2	0.5 M Na_2SO_4 (200 ppm NO_3^-)	1.97	97.46	-0.35	[9]
Ni_{35}/NC-sd	0.5 M Na_2SO_4 （0.3M NO_3^-）	5.1	99	-0.5	[10]
Poly-Cu_{14}cba	0.5 M K_2SO_4 （250 ppm NO_3^-）	2.84	90	-0.15	[11]
Cu_3P NA/CF	0.1 M PBS （0.1 M $NaNO_2$）	1.63	91.2±2.5	-0.5	[12]
Ni_2P/NF	0.1 M PBS （200ppm NO_2^-）	2.69	90.2±3.0	-0.3	[13]
PdCu/Cu_2O	0.2 M Na_2SO_4 （100 ppm NO_3^-)	3.23	94.32	-0.8	[14]
TiO_2 NTs/CuO_x	0.5 M Na_2SO_4 100 ppm KNO_3	1.24	92.23	-0.75	[15]
10Cu/TiO_{2-x}	0.5 M Na_2SO_4 200 ppm $NaNO_3$	1.94	81.34	-0.75	[16]
BP	**0.5 M Na_2SO_4 0.1 M $NaNO_3$**	**3.1**	**96.3**	**-0.8**	**This work**

Supplementary references

[1]. D. Zhu, L. Zhang, R. E. Ruther and R. J. J. N. m. Hamers, *Nat. Mater.*, 2013, **12**, 836-841.

[2]. Y. Wang, C. Wang, M. Li, Y. Yu and B. Zhang, *Chem. Soc. Rev.*, 2021, **50**, 6720-6733.

[3]. L. C. Green, D. A. Wagner, J. Glogowski, P. L. Skipper, J. S. Wishnok and S. R. J. A. b. Tannenbaum, *Anal. Biochem.*, 1982, **126**, 131-138.

[4]. D. Wu, P. Lv, J. Wu, B. He, X. Li, K. Chu, Y. Jia and D. Ma, *J. Mater. Chem. A*, 2023, **11**, 1817-1828.

[5]. J. Li, J. Hu, M. Zhang, W. Gou, S. Zhang, Z. Chen, Y. Qu and Y. Ma, *Nat. Commun.*, 2021, **12**, 3502.

[6]. P. Li, Z. Jin, Z. Fang and G. Yu, *Energy Environ. Sci.*, 2021, **14**, 3522-3531.

[7]. Y. Guo, R. Zhang, S. Zhang, Y. Zhao, Q. Yang, Z. Huang, B. Dong and C. Zhi, *Energy Environ. Sci.*, 2021, **14**, 3938-3944.

[8]. L. Li, C. Tang, X. Cui, Y. Zheng, X. Wang, H. Xu, S. Zhang, T. Shao, K. Davey and S. Z. Qiao, *Angew. Chem., Int. Ed.*, 2021, **133**, 14250-14256.

[9]. Y. Wang, H. Li, W. Zhou, X. Zhang, B. Zhang and Y. Yu, *Angew. Chem., Int. Ed.*, 2022, e202202604.

[10]. P. Gao, Z. H. Xue, S. N. Zhang, D. Xu, G. Y. Zhai, Q. Y. Li, J. S. Chen and X. H. Li, *Angew. Chem., Int. Ed.*, 2021, **133**, 20879-20884.

[11]. Y. M. Wang, J. Cai, Q. Y. Wang, Y. Li, Z. Han, S. Li, C. H. Gong, S. Wang, S. Q. Zang and T. C. Mak, *Angew. Chem., Int. Ed.*, 2022, **134**, e202114538.

[12]. J. Liang, B. Deng, Q. Liu, G. Wen, Q. Liu, T. Li, Y. Luo, A. A. Alshehri, K. A. Alzahrani, D. Ma and X. Sun, *Green Chem.*, 2021, **23**, 5487-5493.

[13]. G. Wen, J. Liang, L. Zhang, T. Li, Q. Liu, X. An, X. Shi, Y. Liu, S. Gao and A. M. Asiri, *J. Colloid Interface Sci.*, 2022, **606**, 1055-1063.

[14]. H. Yin, Z. Chen, S. Xiong, J. Chen, C. Wang, R. Wang, Y. Kuwahara, J. Luo, H. Yamashita and Y. Peng, *Chem Cata.*, 2021, **1**, 1088-1103.

[15]. W. Qiu, X. Chen, Y. Liu, D. Xiao, P. Wang, R. Li, K. Liu, Z. Jin and P. Li, *Appl. Catal., B*, 2022, **315**, 121548.

[16]. X. Zhang, C. Wang, Y. Guo, B. Zhang, Y. Wang and Y. Yu, *J. Mater. Chem. A*, 2022, **10**, 6448-6453.